Res Chem Intermed (2017) 43:401–412
DOI 10.1007/s11164-016-2630-8

Fluorogenic ferrocenyl Schiff base for Zn^{2+} and Cd^{2+} detection

Mukerrem Findik[1] · Asuman Ucar[1] · Haluk Bingol[2] · Ersin Guler[1] · Emine Ozcan[1]

Received: 18 April 2016 / Accepted: 26 June 2016 / Published online: 7 July 2016

Abstract A novel sensor based on acetylferrocene-containing Schiff base (**ASB**) was synthesized by reaction of α-chloroacetylferrocene and *N*-(salicylidene)-L-valinmethylester. The structure of the compound was characterized by using elemental analysis and Fourier-transform infrared (FT-IR), ^{1}H nuclear magnetic resonance (NMR), and ^{13}C NMR spectroscopy. Its metal-cation-sensing properties were investigated spectrofluorometrically. **ASB** served as selective chemosensor for Zn^{2+} and Cd^{2+} towards alkali, alkaline-earth, and various heavy-metal ions. It showed significant fluorescence enhancement for Zn^{2+} and Cd^{2+} ions, stemming from C=N isomerization and chelation-enhanced fluorescence. The binding modes of the complexes were determined to have 1:1 complexation stoichiometry, and the binding constants were calculated as $(6.93 \pm 0.25) \times 10^{6}$ M^{-1} for **ASB·Zn^{2+}** and $(7.49 \pm 0.18) \times 10^{5}$ M^{-1} for **ASB·Cd^{2+}** using the nonlinear curve-fitting method.

Keywords Schiff base · Fluorescence study · Cadmium ion · Zinc ion · Selective metal ion sensor

Introduction

Development of fluorogenic sensors for transition-metal ions is especially attractive due to their excellent sensitivity, simplicity, and rapid response [1–5]. Among transition-metal ions, discrimination of Zn^{2+} and Cd^{2+} has attracted considerable attention from researchers because they occupy the same group of the Periodic Table. Zn^{2+} is an essential cofactor in biological processes, being the second most

✉ Mukerrem Findik
mmukerremm@gmail.com

[1] Department of Chemistry, Faculty of Science, Selcuk University, 42130 Konya, Turkey

[2] Chemistry Department, Ahmet Kelesoglu Education Faculty, Necmettin Erbakan University, 42090 Konya, Turkey

plentiful transition-metal ion in the human body, unlike Cd^{2+}, which plays a different role as a toxic metal ion in biochemical processes [6–10]. However, to date, only a few literature reports are available on applications of fluorescence sensors for zinc and cadmium discrimination [11, 12]. Many researchers have been attracted to develop single chemosensors to distinguish metal ions [9, 13]. They focus on development of simple probes with high reliability, sensitivity, and selectivity, and easy synthesis [14–16].

Several Schiff base fluorescent probes have been developed, because Schiff bases are known to be good ligands due to their selective chelating properties for metal ions [17–20]. C=N isomerization in Schiff bases generally results in weak fluorescence emission due to the attached chromophore, but high-intensity emission can be obtained after this isomerization is stopped by bonding to metal ions [21]. In addition, ferrocene has excellent ability to store electrons, which not only strengthens the coordination between the sensor and metal ion, but also lowers the detection limit of metal ion [22]. Although numerous ferrocene-based sensors for transition-metal ions have been studied [23–26], there are few reports on efficient cation sensing based on simply and easily synthesized Schiff base ferrocene-based sensors [27].

In this work, to explore the selective sensing properties of ferrocenyl Schiff base towards transition-metal ions, a novel acetylferrocene-containing Schiff base (**ASB**) was synthesized. This compound was characterized by elemental analysis and FT-IR, ^{1}H NMR, and ^{13}C NMR spectroscopy. Its metal-ion-sensing properties were also evaluated fluorometrically. The selective sensor properties of compound **ASB** for different metal ions (Na^{+}, Hg^{2+}, Ca^{2+}, Cu^{2+}, Ni^{2+}, Cd^{2+}, Pb^{2+}, Zn^{2+}, Sr^{2+}, Mg^{2+}, Li^{+}, Na^{+}, K^{+}, Rb^{+}, Ag^{+}, Cs^{+}, and Cr^{3+}) were investigated in detail. The results show that compound **ASB** exhibits fluorescent sensor properties for Zn^{2+} and Cd^{2+} in CH_3CN.

Experimental

Materials and methods

L-Valine methylester hydrochloride, salicylaldehyde, ferrocene, chloroacetyl chloride, magnesium sulfate (Mg_2SO_4), and aluminum chloride ($AlCl_3$) were obtained from Sigma-Aldrich and used as received. Petroleum ether, dichloromethane (CH_2Cl_2), triethylamine, and acetonitrile (CH_3CN) were purchased from Merck. All heavy-metal salts were used as perchlorate compounds ($MClO_4$, $M = Na^{+}$, Hg^{2+}, Ca^{2+}, Cu^{2+}, Ni^{2+}, Cd^{2+}, Pb^{2+}, Zn^{2+}, Sr^{2+}, Mg^{2+}, Li^{+}, Na^{+}, K^{+}, Rb^{+}, Ag^{+}, Cs^{+}, and Cr^{3+}) and dried over P_2O_5 prior to use. Melting points were determined on a Büchi B-540 apparatus in sealed capillary and are uncorrected. ^{1}H NMR and ^{13}C NMR spectra were recorded on a Varian 400-MHz spectrometer in $CDCl_3$ and dimethyl sulfoxide (DMSO)-d_6. FT-IR spectra of solid samples were recorded on a PerkinElmer Spectrum 100 FT-IR spectrometer (Universal/ATR sampling accessory). Elemental analyses were performed on a Thermo Flash 2000 Scientific model

analyzer. Fluorescence spectra were measured using a PTI QuantaMaster 400 Fluorometer spectrophotometer at room temperature.

Synthesis of α-chloroacetylferrocene (1)

α-Chloroacetylferrocene was prepared from ferrocene and chloroacetyl chloride in CH_2Cl_2 according to a previously published method [28]. Solution of ferrocene (9.3 g, 50 mmol) in CH_2Cl_2 (40 mL) was added to stirred solution of chloroacetyl chloride (4 mL, 50 mmol) and $AlCl_3$ (7.0 g, 50 mmol) in CH_2Cl_2 (90 mL) at 0 °C under N_2 atmosphere. After 5 h, the solution was extracted three times with water (180 mL), the organic layer was dried with Mg_2SO_4 and concentrated in vacuo, and the residue was subjected to silica gel chromatography (petroleum ether:dichloromethane = 1:10) to afford orange compound **1**. Yield: 17 %, m.p.: 93 °C. ^{1}H NMR (DMSO-d_6, 400 MHz, δ, ppm): 4.85 (t, J = 1.84 Hz, 2H, Cp); 4.76 (s, 2H, CH_2Cl); 4.64 (t, J = 1.84 Hz, 2H, Cp); 4.26 (s, 5H, Cp). IR (cm^{-1}): 1675 (CO). Anal. calcd. for $C_{12}H_{11}ClFeO$: C, 54.85; H, 4.19. Found: C, 54.23; H, 4.82 %.

Synthesis of *N*-(salicylidene)-L-valinmethylester (2)

L-Valine methylester hydrochloride was condensed with salicylaldehyde by the following procedure: Compound **2** was prepared according to literature [29]. Triethylamine (3 mL, 20 mmol) was added to suspension of (L)-valine methylester hydrochloride (20 mmol) in 90 mL dichloromethane. Salicylaldehyde (20 mmol) was added slowly until the color of the reaction mixture turned yellow. The suspension was stirred at room temperature overnight. The solution was washed twice with water, and the organic layer was dried with Mg_2SO_4. The drying agent was filtered off and the filtrate concentrated in vacuo. The remaining yellow oil crystallized while standing at room temperature. Yield 2.71 g (57 %), m.p.: 35 °C. ^{1}H NMR ($CDCl_3$, 400 MHz, δ, ppm): 13.37 (s, 1H, OH); 8.57 (s, 1H, N=CH); 7.49–6.90 (m, 4H, Ar–H); 3.98 (d, 1H, CH); 3.69 (s, 3H, CH_3); 2.27 (m, 1H, CH); 0.91 (d, 3H, CH_3); 0.89 (d, 3H, CH_3). IR (cm^{-1}): 2966, 2874, 2726, 1741, 1627, 1578. Anal. calcd. for $C_{13}H_{17}O_3N$: C, 66.36; H, 7.28; N, 5.95. Found: C, 66.32; H, 7.35; N, 5.83 %.

Synthesis of acetylferrocene-containing Schiff base (ASB)

Compound **2** was condensed with α-chloroacetylferrocene (**1**) by the following procedure (Scheme 1): α-Chloroacetylferrocene (2 mmol) was added to a solution of compound **2** (2 mmol) and triethylamine (0.3 mL, 2 mmol) in 30 mL dichloromethane, and the reaction mixture was stirred at 0 °C under N_2 atmosphere. After 7 h, the solution was extracted three times with water (60 mL), and the organic layer was dried with Mg_2SO_4 and concentrated in vacuo. The remaining dark-red oil crystallized while standing at room temperature. Yield 0.77 g (84 %), m.p.: 54 °C. ^{1}H NMR ($CDCl_3$, 400 MHz, δ, ppm): 8.30 (s, 1H, N=CH); 7.33–6.89 (m, 4H, Ar–H); 4.83 (t, 2H, Cp); 4.60 (t, 2H, Cp); 4.42 (s, 2H, CH_2Cl); 4.25 (s, 5H, Cp); 3.73 (d, 1H, CH); 3.74 (s, 3H, CH_3); 2.37 (m, 1H, CH); 0.97 (d, 3H, CH_3); 0.95 (d, 3H, CH_3). ^{13}C NMR ($CDCl_3$, 100 MHz, δ, ppm): 195.31, 171.56, 166.56,

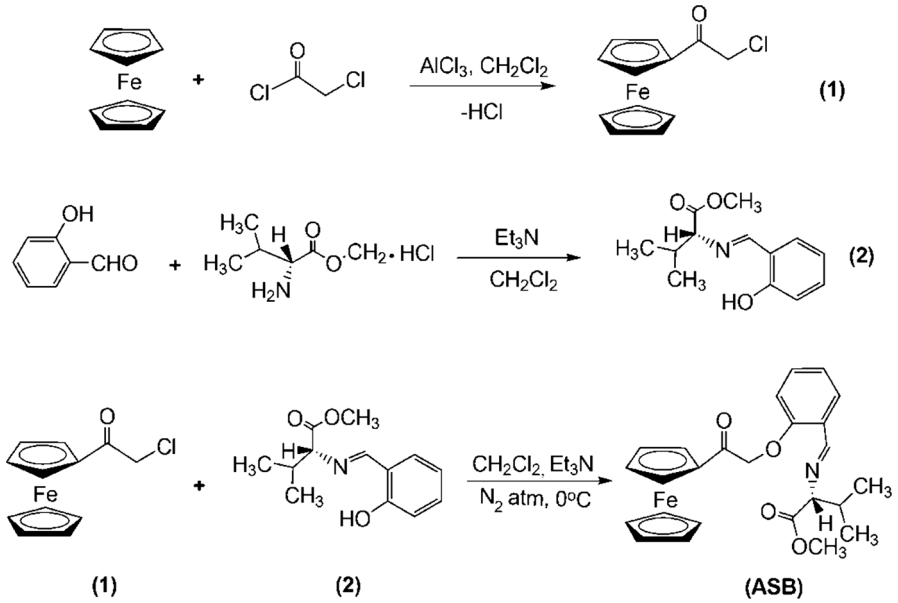

Scheme 1 Synthetic process of **ASB**

161.08, 132.76, 131.69, 118.70, 117.13, 77.93, 75.89, 73.08, 70.18, 69.54, 52.16, 46.08, 31.84, 19.42, 18.18. IR (cm^{-1}): 3029, 2951, 1738, 1681, 1627, 1580, 1169. Anal. calcd. for $C_{25}H_{27}O_4NFe$: C, 65.03; H, 5.85; N, 3.03. Found: C, 65.51; H, 5.34; N, 3.35 %.

Fluorescence studies

To reveal its recognition properties, binding affinity, and sensitivity, the interactions of **ASB** with various metal ions (Hg^{2+}, Ca^{2+}, Cu^{2+}, Ni^{2+}, Cd^{2+}, Pb^{2+}, Zn^{2+}, Sr^{2+}, Mg^{2+}, Li^{+}, Na^{+}, K^{+}, Rb^{+}, Ag^{+}, Cs^{+}, and Cr^{3+}) were systematically investigated by recording the fluorescence response. Stock solutions were prepared by dissolving their hexahydrate perchlorate salts in CH_3CN (5.0×10^{-2} M). The calculated amount of metal solution was added to **ASB** solution, and the final concentrations of the solution were adjusted to the desired value by adding extra CH_3CN. The resulting solution was transferred in a quartz cuvette (3 mL; path length, 1 cm). Fluorescent measurements were recorded after 3 min.

Results and discussion

Structural characterization

The FT-IR spectrum of compound **1** exhibited characteristic absorption bands at 3089 and 1448 cm^{-1}, indicating presence of aromatic C–H and C=C in cyclopentadienyl

ring. The stretching frequency at 1675 cm^{-1} was assigned to C=O vibrations. The other absorptions at 2937 and 779 cm^{-1} were attributed to presence of C–H and C–Cl groups, respectively [28, 30].

FT-IR spectra of aldehydes and amines generally exhibit signals at 1645–1665 cm^{-1} and between 2964 and 3427 cm^{-1}, attributed to C=O and NH_2 stretching vibration. After reaction, a new band was observed at 1627 cm^{-1}, attributed to azomethine (CH=N) group, in the FT-IR spectrum of compound **2**. This finding/change showed that amino and aldehyde groups of the starting reactants converted to corresponding Schiff bases [31]. Other absorption bands were seen at 2966 cm^{-1} for $(C–H)_{arom.}$, 2874 cm^{-1} for $(C–H)_{alph.}$, and 1578 cm^{-1} for (C=C). Vibration of carbonyl group was observed at 1741 cm^{-1} in the amino acid methyl ester [32]. While the O–H stretching frequency of compound **2** was expected in the 3500–3800 cm^{-1} region, this signal was displaced to the 2726 cm^{-1} region due to the O–H···N intramolecular hydrogen bond (Scheme 2). According to this result, the compound is planar in structure, and hence compound **2** has sufficient intramolecular distance to form hydrogen bond [33].

After reaction of compound **1** with compound **2**, the C–Cl (779 cm^{-1}) band disappeared and a new band was observed at 1176 cm^{-1}, attributed to etheric (C–O–C) group, in the FT-IR spectrum of **ASB**. The FT-IR spectra of compounds **2** and **ASB** are shown in Fig. 1.

The ^{1}H NMR and ^{13}C NMR spectra of compounds **1**, **2**, and **ASB** were recorded (solvent, DMSO-d_6 and $CDCl_3$). Detailed structural information was provided by ^{13}C NMR spectra.

In the ^{1}H NMR spectrum of compound **1**, the triplet signals observed in the region 4.64–4.85 ppm and the singlet signal observed at 4.26 ppm were attributed to $–CH_2$ and –CH protons in acetyl and ferrocenyl group, respectively. All protons were found in their expected region [28, 30].

In the ^{1}H NMR spectrum of compound **2**, the singlet signals at 8.57 and 13.37 ppm were attributed to azomethine and phenolic protons, respectively. Aromatic protons in benzene ring were also observed at 7.49–6.90 ppm as multiplet. All of the aliphatic, aromatic, and azomethine carbon (CH=N) shifts were confirmed in the expected regions [29]. Other peaks of **2**, i.e., doublet signal at 3.98 ppm and multiplet signal at 2.27 ppm, and singlet signal at 3.69 ppm and two doublet signals at 0.91–0.89 ppm, were attributed to –CH and $–CH_3$ protons,

Scheme 2 Intramolecular hydrogen bonding in compound **2**

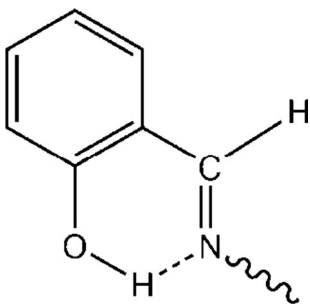

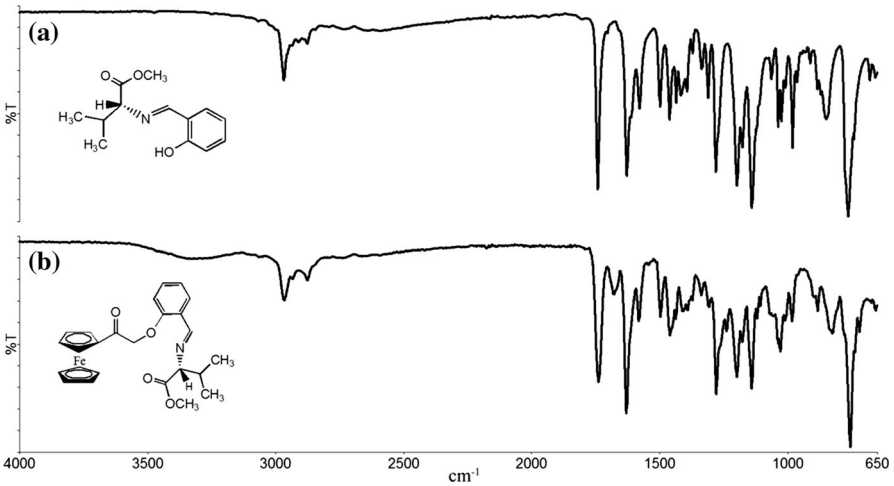

Fig. 1 FT-IR spectra of compound **2** (**a**) and **ASB** (**b**)

respectively (Fig. 2a) [29]. While obtaining **ASB**, phenolic OH band at 13.37 ppm disappeared (Fig. 2b).

The interpretation of the ^{13}C NMR spectrum showed peaks for the various carbon atoms in **ASB** as follows: The azomethine (CH=N) group carbon showed peak at

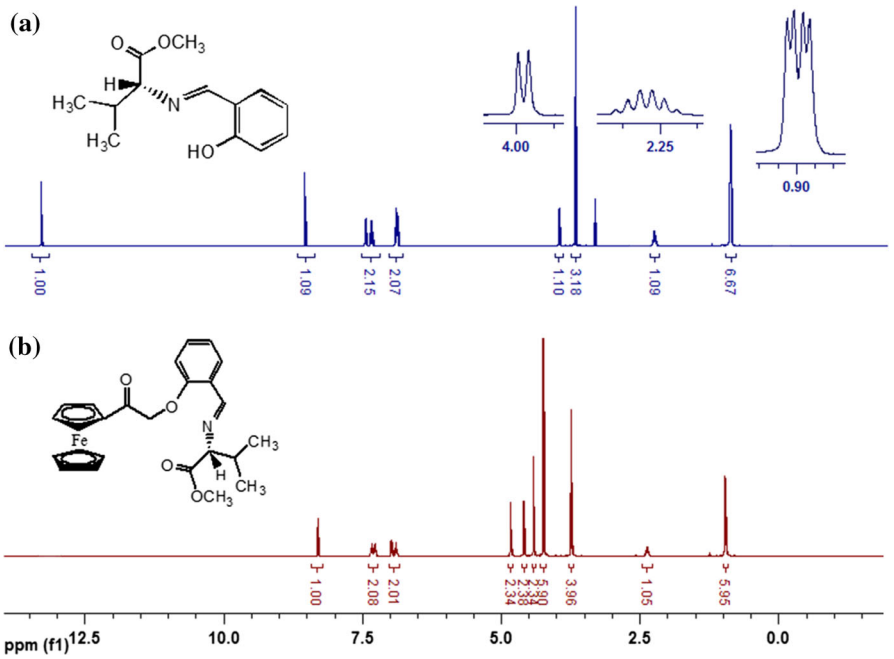

Fig. 2 ^{1}H NMR spectra of compound **2** (**a**) and **ASB** (**b**)

161.08 ppm (Fig. 3). The aromatic carbons in benzene ring showed peak in the range of 132.76–117.13 ppm. The substituted methyl groups in the valine methyl ester exhibited peaks at 52.16, 31.84, and 18.18–19.42 ppm, attributed to O–CH_3 (C_{10}), –CH (C_{11}), and –CH_3 (C_{12}, C_{13}) carbons, respectively [29]. Carbon bonded with carbonyl group exhibited a peak at 171.56 ppm. The signals at 75.89, 73.08, 69.54, 70.18, 195.31, and 46.08 ppm were attributed to C_1, C_2, C_3, C_4, C_5, and C_6 carbons of acetylferrocenyl group, respectively [30].

Fluorescence study

To determine the binding properties of metal ions to **ASB**, the fluorescent response of **ASB** for various metal ions including Hg^{2+}, Ca^{2+}, Cu^{2+}, Ni^{2+}, Cd^{2+}, Pb^{2+}, Zn^{2+}, Sr^{2+}, Mg^{2+}, Li^{+}, Na^{+}, K^{+}, Rb^{+}, Ag^{+}, Cs^{+}, and Cr^{3+} was investigated. **ASB** showed high, substantial change in presence of Zn^{2+} and Cd^{2+} ions. As seen in Fig. 4, **ASB** in CH_3CN showed very weak fluorescence emission with excitation at 378 nm. When 1 equiv of various metal ions such as Hg^{2+}, Ca^{2+}, Cu^{2+}, Ni^{2+}, Cd^{2+}, Pb^{2+}, Zn^{2+}, Sr^{2+}, Mg^{2+}, Li^{+}, Na^{+}, K^{+}, Rb^{+}, Ag^{+}, Cs^{+}, and Cr^{3+} was added, solution of **ASB** exhibited no or small significant increase of fluorescence, except for Cd^{2+} and Zn^{2+}. **ASB** showed selective fluorescence enhancement with Zn^{2+} at 452 nm, even though there was a relatively smaller fluorescence increase with Cd^{2+}. The fluorescence enhancement of **ASB** in presence of Zn^{2+} and Cd^{2+} can be explained by considering the C=N isomerization. Because C=N isomerization in compounds with unbridged C=N structure is the predominant decay process of excited states, such compounds exhibit very poor fluorescence. It is known that compounds containing covalently bridged C=N structure show higher fluorescence

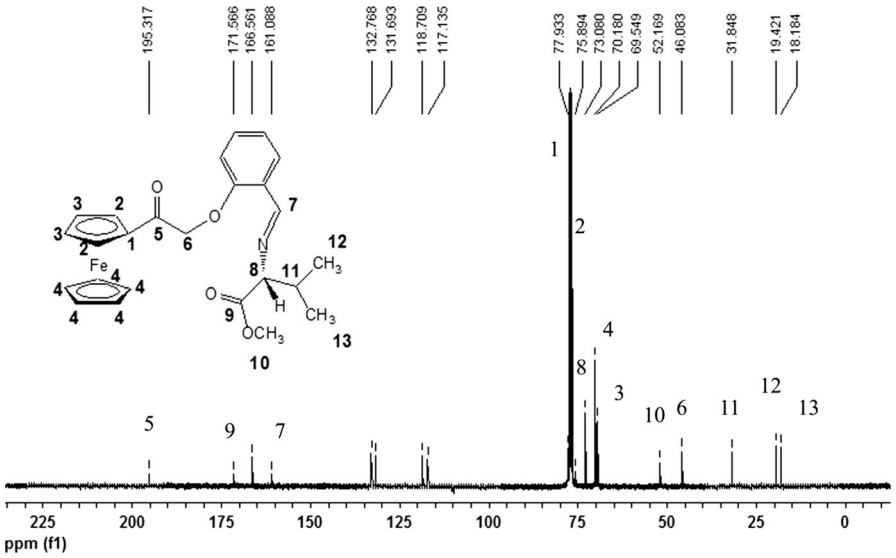

Fig. 3 ^{13}C NMR spectrum of **ASB**

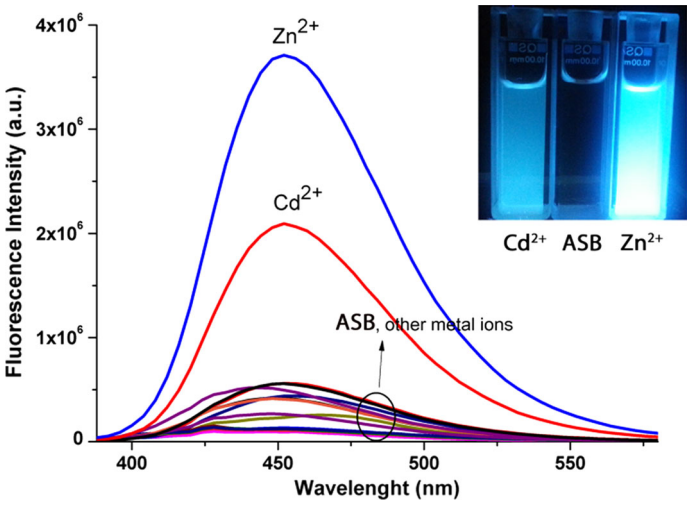

Fig. 4 Fluorescence spectra of **ASB** (5×10^{-6} M) upon addition of different metal ions (1 equiv) in CH_3CN. *Inset* shows photographs of fluorescence response after addition of Zn^{2+} and Cd^{2+} under UV lamp at 365 nm

intensity owing to restriction of C=N isomerization in the excited states [34]. Binding of Zn^{2+} and Cd^{2+} to **ASB** can inhibit C=N isomerization, resulting in a dramatic increase of fluorescence intensity [35]. Chelation of **ASB** with Zn^{2+} and Cd^{2+} can induce rigidity in the complexes, causing a large chelation-enhanced fluorescence (CHEF) effect with drastic enhancement of fluorescence [36]. The CHEF value was determined to be 13 for the case of **ASB**·$\mathbf{Zn^{2+}}$ and 5 for the case of **ASB**·$\mathbf{Cd^{2+}}$.[1] The fluorescence changes under UV lamp (at 365 nm) were also detected by naked eye (Fig. 4, inset). These results indicated that **ASB** can readily distinguish Zn^{2+} and Cd^{2+} from biologically and environmentally relevant metal ions by enhanced fluorescence [37].

The changes in the emission spectrum of **ASB** as a function of Zn^{2+} and Cd^{2+} concentration are shown in Fig. 5. When fluorescent titration was performed with Zn^{2+} or Cd^{2+}, the emission intensity increased up to 10 equiv, then no change was observed. The fluorescence intensity was enhanced almost 12.73-fold upon addition of 10 equiv Zn^{2+} and 4.59-fold upon addition of 10 equiv Cd^{2+}. The fluorescence intensity of **ASB** increased linearly with Zn^{2+} and Cd^{2+} up to 1:1 mol ratio, then remained constant with increasing amount of Zn^{2+} or Cd^{2+}. These changes indicate that **ASB** and the metal ions undergo 1:1 complex formation (Fig. 5a, b, insets) considering the mole fraction method.

Considering the fluorescence changes and complexation ratio (1:1 stoichiometry) between **ASB** and the metal ions at lower equivalents, the nonlinear curve-fitting

[1] The CHEF is defined as I_{max}/I_0, where I_{max} corresponds to the maximum emission intensity of the receptor–metal complex, while I_0 is the maximum emission intensity of the free receptor. For recent and relevant examples of heavy- and transition-metal cation (HTM) chemosensors based on chelation-enhanced fluorescence (CHEF).

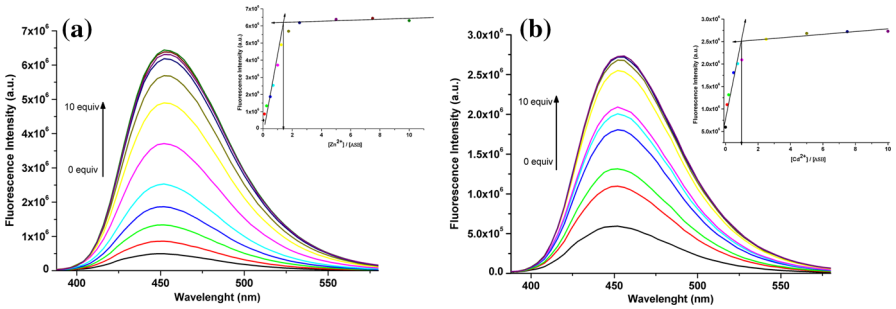

Fig. 5 Fluorescence spectra of **ASB** (5×10^{-6} M) upon addition of **a** Zn^{2+} at 0, 0.1, 0.25, 0.5, 0.75, 1.0, 1.25, 1.75, 2.5, 5.0, 7.5, and 10 equiv, and **b** Cd^{2+} at 0, 0.1, 0.2, 0.5, 0.75, 1.0, 2.5, 5.0, 7.5, and 10 equiv. *Insets* show corresponding titration curves at 452 nm

procedure was used to determine the binding constants (K_a) by applying Eq. (1) [38].

$$r = \frac{I - I^0_{min}}{I^0_{max} - I^0_{min}} + \frac{I - I^0_{min}}{C^0_{min} K_a \left(I^0_{max} - I\right)}, \quad (1)$$

where r is the added equivalents of cation, I^0_{min}, I, and I^0_{max} are the fluorescence of free ligand, ligand plus r equivalents of cation, and ligand plus large excess cation solution, respectively, C^0_{min} is the concentration of free ligand, and K_a is the binding constant. The nonlinear curve fits based on Eq. (1) obtained using Sigma Plot 10.0 are presented in Fig. 6. The binding constant K_a for 1:1 stoichiometry of the complex between **ASB** and the metal ions was calculated as $(1.38 \pm 0.25) \times 10^6$ M^{-1} for **ASB·Zn^{2+}** and $(7.49 \pm 0.18) \times 10^5$ M^{-1} for **ASB·Cd^{2+}** from the curve fitting. These results show that the binding affinity between **ASB** and Zn^{2+} is stronger than that between **ASB** and Cd^{2+}.

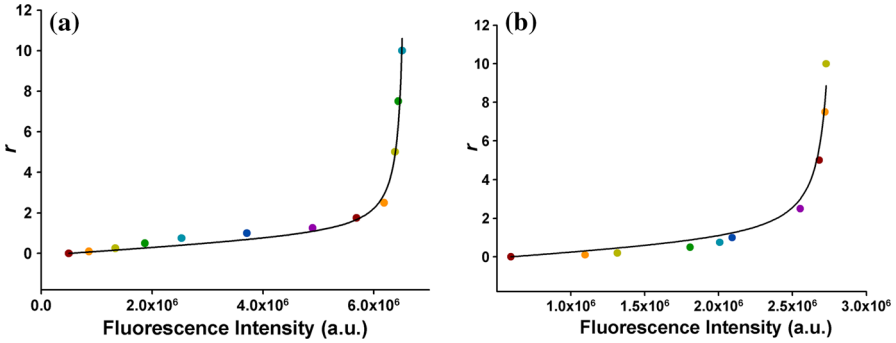

Fig. 6 Nonlinear curve fitting of Eq. (1) for fluorescence change at 452 nm with respect to added amount of **a** Zn^{2+} in the range of 0.1–100 μM (correlation coefficient of the nonlinear curve fitting 0.9910) and **b** Cd^{2+} in the range of 0.5–500 μM (correlation coefficient of nonlinear curve fitting 0.9877)

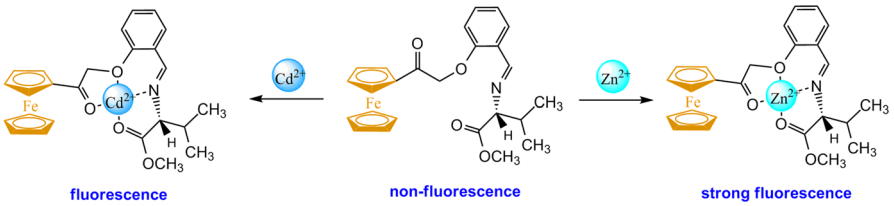

Scheme 3 Proposed structures for **ASB**·$\mathbf{Cd^{2+}}$ and **ASB**·$\mathbf{Zn^{2+}}$ complexes

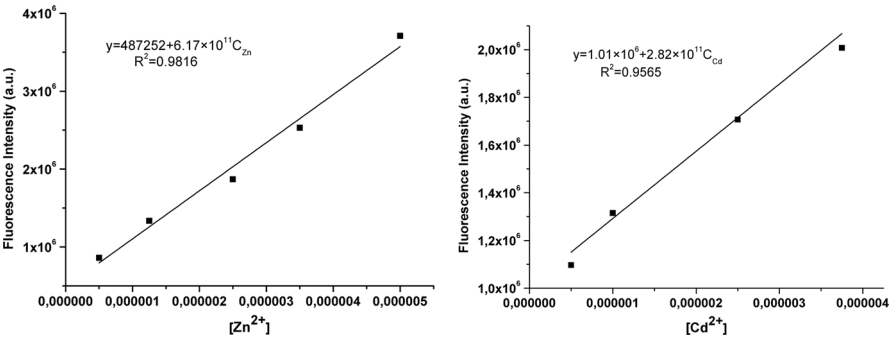

Fig. 7 Calibration curves obtained from plots of fluorescence intensity (at 365 nm for Zn^{2+} and Cd^{2+}) with added Zn^{2+} and Cd^{2+} concentration in CH_3CN

Considering the results for the stoichiometric ratio and binding constants, structures for the **ASB**·$\mathbf{Cd^{2+}}$ and **ASB**·$\mathbf{Zn^{2+}}$ complexes are proposed in Scheme 3.

To calculate the detection limit, calibration curves were obtained from plots of fluorescence intensity versus added Zn^{2+} and Cd^{2+} concentration (Fig. 7). The detection limit for Zn^{2+} and Cd^{2+} was determined to be 0.68 and 0.94 μM, respectively, according to DL = $3.3\sigma/S$.[2] These results clearly demonstrate that **ASB** was highly efficient in sensing Zn^{2+} or Cd^{2+}. The reversibility of the sensor was also examined. The fluorescence intensity decreased almost to that of bare **ASB** when 10 μM ethylenediaminetetraacetic acid (EDTA) was added to solution of **ASB**·$\mathbf{Zn^{2+}}$ and **ASB**·$\mathbf{Cd^{2+}}$. These results show that compound **ASB** could be regenerated for repeated use as an optical sensor.

Conclusions

We describe herein preparation of a novel acetylferrocene-containing Schiff base (**ASB**) and characterization of its structure by using elemental and spectroscopic (FT-IR, ^{1}H NMR, ^{13}C NMR) methods. **ASB** displayed selective and sensitive fluorescence response to Zn^{2+} and Cd^{2+} in CH_3CN. Addition of Zn^{2+} and Cd^{2+}

[2] Guidance for industry Q2B validation of analytical procedures: methodology, Nov 1996.

showed drastic enhancement of emission intensity, meaning that **ASB** could be used as a dual sensor in CH_3CN for these metal ions. In other words, **ASB·Zn^{2+}** showed high fluorescence enhancement, even though **ASB·Cd^{2+}** showed relatively smaller fluorescence increase. The binding modes of Zn^{2+} and Cd^{2+} to **ASB** were examined by nonlinear curve fitting, proving that **ASB** coordinates with the metal ions in a 1:1 complex. Simultaneously, chelation between the ligand and metal ion causes a large CHEF effect, which induces the increase of fluorescence intensity. In particular, **ASB** can detect Zn^{2+} selectively in CH_3CN in presence of other metal ions, except Cd^{2+} ion. This sensitive and selective fluorescent sensor can provide guidance for the development of new chemosensors.

Acknowledgments This work was supported by Scientific Research Projects (BAP 13201019) of Selcuk University.

References

1. M. Kaur, P. Kaur, V. Dhuna, S. Singh, K. Singh, Dalton Trans. **43**, 5707–5712 (2014)
2. S. Maiti, Z. Aydin, Y. Zhang, M. Guo, Dalton Trans. **44**, 8942–8949 (2015)
3. B. Sen, M. Mukherjee, S. Banerjee, S. Pal, P. Chattopadhyay, Dalton Trans. **44**, 8708–8717 (2015)
4. S. Anbu, R. Ravishankaran, M.F.C.G. Da Silva, A.A. Karande, A.J.L. Pombeiro, Inorg. Chem. **53**, 6655–6664 (2014)
5. V.K. Gupta, N. Mergu, L.K. Kumawat, A.K. Singh, Sens. Actuators B **207**, 216–223 (2015)
6. J. Wang, W. Lin, W. Li, Chem. Eur. J. **18**, 13629–13632 (2012)
7. S.K. Lee, M.G. Choi, J. Choi, S.K. Chang, Sens. Actuators B **207**, 303–307 (2015)
8. Q. Zhao, R. Li, S. Xing, X. Liu, T. Hu, X. Bu, Inorg. Chem. **50**, 10041–10046 (2011)
9. Z. Liu, C. Zhang, W. He, Z. Yang, X. Gao, Z. Guo, Chem. Commun. **46**, 6138–6140 (2010)
10. V.K. Gupta, M.R. Ganjali, P. Norouzi, H. Khani, A. Nayak, S. Agarwal, Crit. Rev. Anal. Chem. **41**, 282–313 (2011)
11. F. Xiao, J. Shen, J. Qu, S. Jing, D.R. Zhu, Inorg. Chem. Commun. **35**, 69–71 (2013)
12. J.T. Hou, B.Y. Liu, K. Li, K.K. Yu, M.B. Wu, X.Q. Yu, Talanta **116**, 434–440 (2013)
13. Y. Ma, F. Wang, S. Kambam, X. Chen, Sens. Actuators B **188**, 1116–1122 (2013)
14. K. Dutta, R.C. Deka, D.K. Das, Spectrochim. Acta A **124**, 124–129 (2014)
15. R. Borthakur, U. Thapa, M. Asthana, S. Mitra, K. Ismail, R.A. Lal, J. Photochem. Photobiol. A Chem. **301**, 6–13 (2015)
16. B. Kashyap, K. Dutta, D.K. Das, P. Phukan, J. Fluoresc. **24**, 975–981 (2014)
17. H. Ye, F. Ge, Y.M. Zhou, J.T. Liu, B.X. Zhao, Spectrochim. Acta A **112**, 132–138 (2013)
18. J.H. Hu, J.B. Li, J. Qi, Y. Sun, Sens. Actuators B **208**, 581–587 (2015)
19. R. Pandey, R.K. Gupta, M. Shahid, B. Maiti, A. Misra, D.S. Pandey, Inorg. Chem. **51**, 298–311 (2011)
20. V.K. Gupta, A.K. Singh, L.K. Kumawat, Sens. Actuators B **195**, 98–108 (2014)
21. L. Wang, H. Li, D. Cao, Sens. Actuators B **181**, 749–755 (2013)
22. Y.S. Mi, Z. Cao, Y.T. Chen, Q.F. Xie, Y.Y. Xu, Y.F. Luo, J.J. Shic, J.N. Xiang, Analyst **138**, 5274–5280 (2013)
23. C.K. Kumar, R. Trivedi, L. Giribabu, S. Niveditha, K. Bhanuprakash, B. Sridhar, J. Organomet. Chem. **780**, 20–29 (2015)
24. P. Chinapang, V. Ruangpornvisuti, M. Sukwattanasinitt, P. Rashatasakhon, Dyes Pigments **112**, 236–238 (2015)
25. J. Shen, T. Liu, Y. Li, W. Ji, S. Jing, D.R. Zhu, G.F. Guan, Inorg. Chem. Commun. **44**, 6–9 (2014)
26. S.J. Ponniah, S.K. Barik, A. Thakur, R. Ganesamoorthi, S. Ghosh, Organometallics **33**, 3096–3107 (2014)
27. V. Uahengo, B. Xiong, P. Zhao, Y. Zhang, P. Cai, K. Hu, G. Cheng, Sens. Actuators B **190**, 937–945 (2014)
28. L. Zhu, D. Zhang, D. Qu, Q. Wang, X. Ma, H. Yian, Chem. Commun. **46**, 2587–2589 (2010)

29. G. Warncke, U. Böhme, B. Günther, M. Kronstein, Polyhedron **47**, 46–52 (2012)
30. O. Dogan, V. Senol, S. Zeytinci, H. Koyuncu, A. Bulut, J. Organomet. Chem. **690**, 430–434 (2005)
31. M.L. Sundararajan, T. Jeyakumar, J. Anandakumaran, B.K. Selvan, Spectrochim. Acta A **131**, 82–93 (2014)
32. J. Müller, G. Kehr, R. Fröhlich, G. Erker, Eur. J. Inorg. Chem. **2005**, 2836–2841 (2005)
33. D. Tomczyk, L. Nowak, W. Bukowski, K. Bester, P. Urbaniak, G. Andrijewski, B. Olejniczak, Electrochim. Acta **121**, 64–77 (2014)
34. J. Wu, W. Liu, J. Ge, H. Zhang, P. Wang, Chem. Soc. Rev. **40**, 3483–3495 (2011)
35. Y.J. Lee, C. Lim, H. Suh, E.J. Song, C. Kim, Sens. Actuators B **201**, 535–544 (2014)
36. L. Wang, W. Qin, X. Tang, W. Dou, W. Liu. J. Phys. Chem. A **115**, 1609–1616 (2011)
37. X. Liu, N. Zhang, J. Zhou, T. Chang, C. Fangab, D. Shangguan, Analyst **138**, 901–906 (2013)
38. H. Bingol, E. Kocabas, E. Zor, A. Coskun, Talanta **82**, 1538–1542 (2010)